

Surface conductivity for Au or Ag on Si(111)

Chun-Sheng Jiang,* Shuji Hasegawa, and Shozo Ino

Department of Physics, School of Science, University of Tokyo, Hongo, Bunkyo-ku, Tokyo, 113, Japan

(Received 26 December 1995; revised manuscript received 28 May 1996)

The surface electrical conductivity was separated from the bulk one by simultaneous conductivity measurements of two different surface structures formed on a single Si-wafer surface in ultrahigh vacuum. We have found that the surface conductivities for the Si(111)- $\sqrt{3}\times\sqrt{3}$ -Ag and 5×2 -Au superstructures are inherently higher than that of the Si(111)- 7×7 clean surface by $(11.5\pm 0.5)\times 10^{-5}$ A/V and $(5\pm 1)\times 10^{-5}$ A/V, respectively. These excess conductivities are estimated to originate mainly from the surface space-charge layer, although the surface-state-band conduction is considered to partly contribute, especially on the $\sqrt{3}\times\sqrt{3}$ -Ag surface. [S0163-1829(96)00940-X]

Electrical conduction at semiconductor surface has been studied as a macroscopic property for more than 50 years as one of the main subjects in semiconductor physics, especially in its early days. Until recently, however, it was not achieved to investigate the conductance for atomically-ordered surfaces, for which the ultrahigh-vacuum (UHV) condition is essentially important. For the changes of conductance caused by metal-layer growth on the surface, Henzler and co-workers concluded that the increases of conductance during Ag growth on the Si(111)- 7×7 surface at low temperatures corresponded to the metal percolations.¹ Hasegawa and Ino deposited metals (Ag, Au, In) onto various substrate-surface structures [Si(111)- 7×7 , $-\sqrt{3}\times\sqrt{3}$ -Ag, etc.] at room temperature (RT), and found that the changes of conductance at beginning of depositions were crucially dependent on the surface structures.² This phenomenon was tentatively attributed to the effects of the band bending below the surface, which was governed by the surface atomic and electronic structures.

However, the absolute values of the surface conductivity with these well-defined structures, as a fundamental property of the surfaces, remain unknown. Its measurements are not straightforward because the concentration and distribution of dopants in the bulk may change by high-temperature heating,^{3,4} which is generally necessary for making a superlattice surface structure such as the Si(111)- 7×7 and $-\sqrt{3}\times\sqrt{3}$ -Ag, etc., resulting in the change of both surface and bulk conductivities. To extract the surface contribution from the measured conductivity, we made two surface structures simultaneously on a single Si(111) wafer surface, and measured the conductivities of the respective surface areas. The bulks beneath them had the same temperature and heating histories, resulting in the same bulk conductivities. So the difference in the measured conductivity could be attributed only to the difference in the surface conductivity. Furthermore, by measuring ultraviolet and x-ray photoelectron spectra (UPS and XPS) for these surfaces, and also by using the data in the literature, the excess surface conductivities are discussed in terms of the surface space-charge layer and surface-state bands.

Figure 1 shows a schematic illustration of the sample holder for the conductivity measurements and reflection high-energy electron diffraction (RHEED) observations. The

Si(111) wafer (*p*-type, resistivity of 20 Ω cm) with its size of $40\times 5\times 0.4$ mm³ was heated by direct electric currents. The heating temperatures and cooling processes for preparing the 7×7 clean surface were as follows: flashed at 1200 $^{\circ}$ C for 5 sec, slowly cooled down to 780 $^{\circ}$ C in 3 min, annealed at 780 $^{\circ}$ C for 3 min, and finally cooled down to RT in 3 min. The flashing up to 1200 $^{\circ}$ C is known to be necessary to remove C contaminations, which were checked by the XPS and RHEED. The longer annealing at 780 $^{\circ}$ C was effective to make a larger domain size for the 7×7 structure.⁵ Since domain boundaries may affect the surface conductivity, a large domain size will be favorable to investigate a surface as ideally as possible. The temperature above 700 $^{\circ}$ C was measured with an optical pyrometer, while the temperature below it was determined through extrapolation using the relationship between the heating current and the temperature.⁶ The central portion of the Si wafer, where the resistance was measured, was almost uniformly heated, while both areas close to the Ta-end clamps had lower temperatures. The $\sqrt{3}\times\sqrt{3}$ -Ag and 5×2 -Au structures were

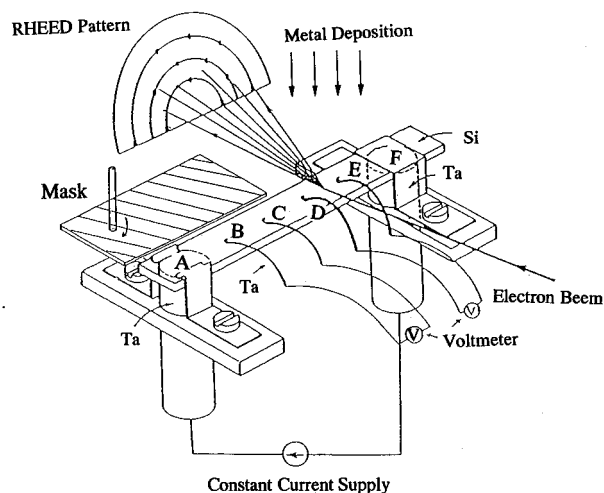


FIG. 1. A schematic illustration of the sample holder for the surface-conductivity measurement and reflection high-energy electron diffraction (RHEED) observations. After confirming the surface structures by RHEED, the electron beam was turned off during the following conductivity measurements.

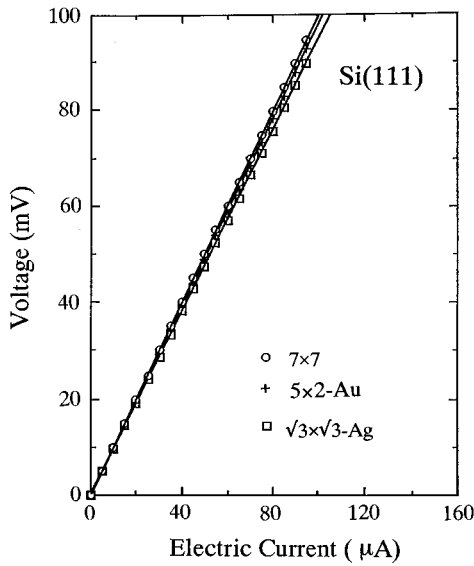


FIG. 2. An example of the conductivity measurements for the Si(111)7×7, $\sqrt{3}\times\sqrt{3}$ -Ag, and 5×2 -Au structures from the linear relation between voltage signals and currents.

made at the substrate temperature of 510 °C by Ag deposition of 1 ML (monolayer) with a rate of 0.4 ML/min, and at 680 °C by Au deposition of 0.4 ML with a rate of 0.4 ML/min, respectively. Higher annealing temperatures were selected from the phase diagrams of these surface structures.^{7,8} to make larger domains. During the metal depositions, a half of the wafer (*BC*) was covered by a mask to prevent the metal adsorption, while both regions (*BC* and *DE*) were annealed at a uniform temperature. The structure of another half surface (*DE*) deposited with metal (Ag or Au) was changed gradually to the $\sqrt{3}\times\sqrt{3}$ -Ag or 5×2 -Au, while the masked area (*BC*) remained the clean 7×7 structure.

Before the conductivity measurements, the condition of the electrical contact between the substrate and the Ta wire electrodes (*B,C*) and (*D,E*) was confirmed by observing a linear relation between voltage signals and electrical currents. First, the resistances of the both areas, R_{BC}^0 and R_{DE}^0 , were measured at RT with the same 7×7 structures before metal depositions. Because of their same bulk resistivity, the ratio of the distances between the respective two contacts was determined as $P = \overline{DE}/\overline{BC} = R_{DE7\times 7}^0/R_{BC7\times 7}^0$. After making the $\sqrt{3}\times\sqrt{3}$ -Ag or 5×2 -Au structure on the *DE* side, the resistance $R_{BC7\times 7}$ on the masked side *BC* occasionally changed a little because of the additional heat treatments. Then, the corresponding resistance of the 7×7 on the *DE* side should be $R_{DE7\times 7} = P \times R_{BC7\times 7}$. The measured resistances of the $\sqrt{3}\times\sqrt{3}$ -Ag and 5×2 -Au, $R_{DE\sqrt{3}\times\sqrt{3}}$ and $R_{DE5\times 2}$, were compared with this corresponding value of the 7×7 on the same *DE* side, $R_{DE7\times 7}$. dc electric current up to 95 μA through the sample was changed with step of 5 μA , and linear current-voltage relations were fitted with the least-square method. Because the heat conduction was very slow in UHV environment, it took more than 2 h for the sample to cool down to RT to attain a stable resistance after the surface structures were prepared at high temperatures.

Figure 2 shows an example of the measurements for these

three surface structures (the data for the 7×7 are the corresponding ones of the *DE* contacts $R_{DE7\times 7}$). By averaging several measurements like Fig. 2, the conductivities σ for the 7×7, $\sqrt{3}\times\sqrt{3}$ -Ag, and 5×2 -Au surfaces were determined to be 5.06, 5.35, and $5.18\times 10^{-2} \Omega^{-1} \text{cm}^{-1}$, respectively. Since their bulk conductivities σ_b are the same, it is concluded that the $\sqrt{3}\times\sqrt{3}$ -Ag and 5×2 -Au have larger contributions of surface conductivity than the 7×7 surface. The conductivity σ including both of the bulk and surface contributions is given by

$$\sigma = \int_0^d [\sigma_s(z) + \sigma_b] dz/d,$$

$$\bar{\sigma}_s = \int_0^d \sigma_s(z) dz = (\sigma - \sigma_b)d,$$

where σ_b [$\Omega^{-1} \text{cm}^{-1}$] and $\bar{\sigma}_s$ [Ω^{-1}] are the bulk and surface conductivities, respectively, and d is the thickness of the wafer ($d=0.4 \text{ mm}$). Then, the difference in the surface conductivities between the two surface structures is obtained just from the both measured conductivities: $\bar{\sigma}_{s1} - \bar{\sigma}_{s2} = (\sigma_1 - \sigma_2)d$. Thus,

$$\bar{\sigma}_s(\sqrt{3}\times\sqrt{3}) - \bar{\sigma}_s(7\times 7) = (11.5 \pm 0.5) \times 10^{-5} \text{ A/V},$$

$$\bar{\sigma}_s(5\times 2) - \bar{\sigma}_s(7\times 7) = (5 \pm 1) \times 10^{-5} \text{ A/V},$$

where $\bar{\sigma}_s(7\times 7)$, $\bar{\sigma}_s(\sqrt{3}\times\sqrt{3})$, and $\bar{\sigma}_s(5\times 2)$ means the surface conductivity of the 7×7, $\sqrt{3}\times\sqrt{3}$ -Ag, and 5×2 -Au structures, respectively.

We now discuss the reasons why the $\sqrt{3}\times\sqrt{3}$ -Ag and 5×2 -Au surfaces have higher conductivities than the 7×7 clean surface. For clean and metal-covered semiconductor surfaces, in general, the electrical conduction through the surface region is divided into three types: (1) through the surface space-charge layer, (2) through the grown-metal thin layer, and (3) through the two-dimensional bands of the surface electronic states.⁹

We first estimate the contribution of the surface space-charge layer. Since the measured conductivity of the Si wafer with the 7×7 structure was $5.06\times 10^{-2} \Omega^{-1} \text{cm}^{-1}$ which was consistent with the initial resistivity of 20 Ωcm , the doping profile near the surface region of our *p*-type samples was not considered to be significantly changed by the high-temperature treatments. The hole or impurity concentration is then estimated to be $1.86\times 10^{15} \text{cm}^{-3}$ by using the hole mobility of its bulk values (495 $\text{cm}^2/\text{V s}$). The Fermi-level (E_F) position in the bulk is then estimated to be located at 0.29 eV above the valence-band maximum (VBM). If the E_F positions at both sides of the surface space-charge layer, i.e., at the surface and in the interior bulk, are given as the boundary conditions, the electrical field (band bending) and carrier density in the surface space-charge layer can be calculated by solving the Poisson equation by assuming a uniform distribution of impurity throughout the layer. The conductivity through the layer was then calculated,¹⁰ using the bulk parameters of the hole mobility, 495 $\text{cm}^2/\text{V s}$, and the electron mobility, 1330 $\text{cm}^2/\text{V s}$. The result is shown in Fig. 3 as a function of the surface E_F position. It is known that the surface E_F of the 7×7 structure lies at 0.63 eV above the

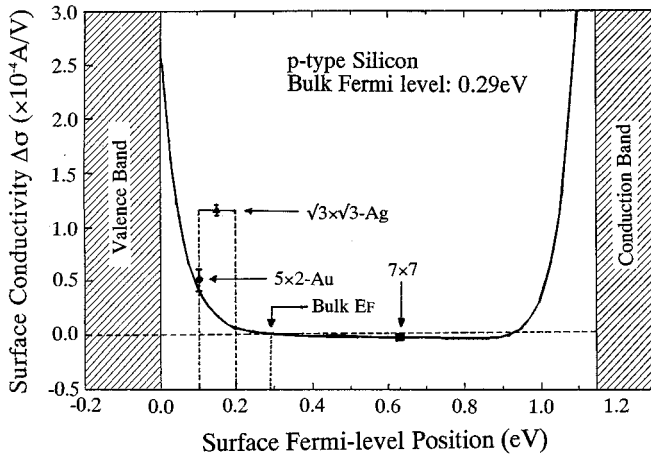


FIG. 3. A calculated conductivity through the surface space-charge layer as a function of the surface Fermi-level position with respect to the valence-band maximum. The ordinate indicates the excess conductivity with respect to the flat-band condition. The surface E_F positions measured by soft x-ray photoemission spectroscopy (Refs. 12–14) and our data of the surface conductivity of the $\sqrt{3} \times \sqrt{3}$ -Ag and 5×2 -Au surfaces are plotted.

VBM, irrespective of the bulk impurity concentration.¹¹ This means a very low conductivity through the surface space-charge layer from Fig. 3, i.e., a depletion layer below the 7×7 structure. According to the high-resolution measurements of Si $2p$ core-level shift using soft x-ray photoemission spectroscopy (PES) between the 5×2 -Au and the clean 7×7 surfaces,¹² the E_F position on the 5×2 -Au surface should lie at 0.10 eV above the VBM. By plotting this E_F position on Fig. 3, the conductivity should increase by about 4×10^{-5} A/V compared with the 7×7 surface. This value seems consistent with our measured excess conductivity, $(5 \pm 1) \times 10^{-5}$ A/V. Therefore it can be said that the excess surface electrical conductivity for the 5×2 -Au structure is mainly attributed to the surface space-charge layer. Since, however, our estimation of the curve in Fig. 3 is based on unrefined assumptions (uniform distribution of the dopants and the bulk-mobility values), the contribution of the conduction through the surface-state band cannot be ruled out at present, as discussed later.

For the $\sqrt{3} \times \sqrt{3}$ -Ag surface, again, the soft x-ray PES measurements for Si $2p$ core-level shift indicate that the surface E_F lies at 0.10 eV (Ref. 13) or 0.20 eV (Ref. 14) above the VBM. Then, the excess conductivity estimated from Fig. 3 is 4×10^{-5} A/V or less, which is too small to explain our measured value, 1.1×10^{-4} A/V. Though this discrepancy may partly come from the unrefined assumption for the estimation of the curve in Fig. 3 as mentioned above, we need other reasons to explain the larger discrepancy compared with the 5×2 -Au case. The surface-state-band conductivity seems to have a larger contribution on this surface as discussed below.

We next discuss the contribution of two other types of conduction, i.e., through the grown-metal layer and through the surface-state bands. According to a recent structural model of the 5×2 -Au surface,¹⁵ the saturation coverage of Au for this phase is 0.4 ML, which is too small to be regarded as a metal Au layer grown on the surface. In fact, the

angle-resolved UPS (ARUPS) data show a peculiar feature which intrinsically originates from the 5×2 superstructure; metallic edges in a restricted range of the emission angle are seen.¹⁶ Collins *et al.*¹⁷ suggest a quasi-one-dimensional metallic character of this surface on the basis of their ARUPS measurements. So there is a possibility that a part of the excess surface electrical conductivity of the 5×2 -Au surface is attributed to this quasi-one-dimensional metallic surface state; the conductivity can be enhanced along the stripes with fivefold-units separation observed in images of scanning tunneling microscopy.¹⁸ But, as mentioned above, this contribution could not be confirmed by our measurements and analysis, probably because our sample surfaces were composed of mixture of the 5×2 -structure domains with three different orientations.

According to the honeycomb-chained-trimer model of the $\sqrt{3} \times \sqrt{3}$ -Ag structure,^{19,20} 1 ML Ag atoms form covalent bonds with the substrate Si atoms, which are essentially different from metallic bonds in Ag bulk. This is actually shown in the ARUPS (Ref. 21) and the inverse PES,²² which indicate a distinct energy gap around the E_F in the surface-state band structure. However, Johansson *et al.*¹⁴ report a strongly dispersive surface-state (S_1 state) band crossing the E_F . Only 2.5% of the band is occupied by electrons in neutral balance with the dopant ions in the bulk. This is, however, not a metallic band, but is observed due to the extremely high-doping concentration of their n -type Si wafer. The surface electronic state is inherently semiconductorlike. This S_1 -state band, of which minimum is close to the E_F at the $\bar{\Gamma}$ point in the surface Brillouin zone, is reproduced by the first-principles calculations.²³ Since our sample was a lightly-doped one, our *in situ* ARUPS measurements did not show any photoemission intensity at the E_F over the Brillouin zone as in the previous reports.²¹ This is because the minimum of the S_1 band is above the E_F so that the number of the electrons thermally excited into this surface-state band are not enough to give rise to the photoemission intensity. But these electrons can contribute to the electrical conduction, because the S_1 -state band is highly dispersive. So for the $\sqrt{3} \times \sqrt{3}$ -Ag surface, the measured excess conductivity beyond the calculated curve in Fig. 3 is considered to be attributed to this surface-state band. The surface charging, which is the origin of the upward band bending below this surface, is naturally understood by considering the excess electrons in this S_1 surface-state band.¹⁴

We have found a phenomenon indicative of another reason for the excess surface conductivity of the $\sqrt{3} \times \sqrt{3}$ -Ag surface, which is not necessarily incompatible with the surface-state conduction mentioned above. When we deposited the very small amount of additional Ag atoms (less than 0.03 ML) onto the $\sqrt{3} \times \sqrt{3}$ -Ag surface at RT, the individual adatoms continued to exist as a two-dimensional gas phase with high mobility.²⁴ This situation made the resistance of the Si wafer extremely low. So it is considered that some amount of dilute Ag adatoms layer is formed on top of the $\sqrt{3} \times \sqrt{3}$ -Ag surface under an equilibrium at RT, which raises the excess electrical conductivity. The existence of this dilute Ag adatom phase and its effect on the surface electronic state is already noted in the literature.^{14,25} But it is not yet clear why the dilute Ag adatoms enhance the conductivity.

ity. We just speculate that the adatoms donate the electrons into the S_1 surface-state band, leading to the enhancement of the surface-state conduction through the S_1 band as well as the conduction through the surface space-charge layer due to the enhanced upward band bending.

Finally we should comment on the surface electronic structure of the 7×7 clean surface. This surface is well known to be metallic due to the dangling bonds of the top-most surface atoms.²⁶ But its surface conductivity was lower than that of the $\sqrt{3}\times\sqrt{3}$ -Ag surface, of which electronic structure is inherently semiconductor-like. This means that the conduction via the metallic surface-state band of the 7×7 structure is not high enough to surpass the excess conductivities through the surface space-charge layer and the surface-state S_1 band of the $\sqrt{3}\times\sqrt{3}$ -Ag surface. This may be because the dispersion of the metallic band of the 7×7 surface is so small (less than 0.1 eV) that the electrons with a large effective mass in the band are almost localized on the dangling bonds of the surface atoms.

In conclusion, the surface conductivities for the Si(111)- $\sqrt{3}\times\sqrt{3}$ -Ag and 5×2 -Au structures were measured to be

larger than that of the 7×7 clean surface. This result was qualitatively confirmed also with n -type Si wafers. We have thus found that the reconstructions only in one or two atomic layers on the surface actually raise the inherent changes in the macroscopic electrical conduction. The excess conductivities were explained mainly through the surface space-charge layer. But the surface-state band conduction is considered to partly contribute, especially on the $\sqrt{3}\times\sqrt{3}$ -Ag surface. In spite of a report insisting the detection of the surface-state conduction on the 7×7 surface,²⁷ we could not confirm its contribution. The conductivity measurements as a function of the sample temperature, especially in the low-temperature region, will be effective to fully characterize the mechanisms of the surface conductivity which are now in progress.

The authors acknowledge S. Shimokoshi for his help in manufacturing the electronic circuits. This work was supported by a Grant-In-Aid from the Ministry of Education, Science and Culture of Japan, and also the Sumitomo Foundation.

*Present address: Surface and Interface Laboratory, The Institute of Physical and Chemical Research, Wako, Saitama, 351-01, Japan.

¹R. Schad, S. Heun, T. Heidenblut, and M. Henzler, Phys. Rev. B **45**, 11 430 (1992).

²S. Hasegawa and S. Ino, Phys. Rev. Lett. **68**, 1192 (1992); Surf. Sci. **283**, 438 (1993); Thin Solid Films **228**, 113 (1993); Int. J. Mod. Phys. B **7**, 3817 (1993).

³H. Li and H. Yasunaga, Jpn. J. Appl. Phys. **24**, 928 (1985).

⁴M. Liehr *et al.*, J. Appl. Phys. **61**, 4619 (1987).

⁵W. Telieps and E. Bauer, Surf. Sci. **162**, 163 (1985).

⁶T. Ichikawa and S. Ino, Surf. Sci. **105**, 395 (1981).

⁷Y. Gotoh and S. Ino, Jpn. J. Appl. Phys. **17**, 2097 (1978).

⁸S. Ino, Jpn. J. Appl. Phys. **16**, 891 (1977); in *Reflection High-Energy Electron Diffraction and Reflection Electron Imaging of Surfaces*, edited by P. K. Larsen and P. J. Dobson (Plenum, New York, 1988), p. 3.

⁹For a review, see M. Henzler, in *Surface Physics of Materials I*, edited by J.M. Blakely (Academic Press, New York, 1975), p. 241.

¹⁰C.E. Young, J. Appl. Phys. **32**, 329 (1961).

¹¹F.J. Himpsel, G. Hollinger, and R.A. Pollack, Phys. Rev. B **28**, 7014 (1983).

¹²T. Okuda, H. Daimon, H. Shigeoka, S. Suga, T. Kinoshita, and A. Kakizaki, J. Electron Spectrosc. Relat. Phenom. (to be published).

¹³S. Kono, K. Higashiyama, T. Kinoshita, H. Kato, H. Ohsawa, and

Y. Enta, Phys. Rev. Lett. **58**, 1555 (1987).

¹⁴L.S.O. Johansson, E. Landemark, C.J. Karlsson, and R.I.G. Uhrberg, Phys. Rev. Lett. **63**, 2092 (1989); **69**, 2451 (1992).

¹⁵L.D. Marks and R. Plass, Phys. Rev. Lett. **75**, 2172 (1995).

¹⁶Y. Tezuka, Doctor thesis, University of Tokyo, 1991.

¹⁷I.R. Collins, J.T. Moran, P.T. Andrews, R. Cosso, J.D. O'Mahony, J.F. McGilp, and G. Margaritondo, Surf. Sci. **325**, 45 (1995).

¹⁸A.A. Baski, J. Nogami, and C.F. Quate, Phys. Rev. B **41**, 10 247 (1990).

¹⁹T. Takahashi and S. Nakatani, Surf. Sci. **282**, 17 (1993), and references therein.

²⁰M. Katayama, R.S. Williams, M. Kato, E. Nomura, and M. Aono, Phys. Rev. Lett. **66**, 2762 (1991).

²¹T. Yokotsuka, S. Kono, S. Suzuki, and T. Sagawa, Surf. Sci. **127**, 35 (1983).

²²J.M. Nicholls, F. Salvan, and B. Reihl, Phys. Rev. B **34**, 2945 (1986).

²³Y.G. Ding, C.T. Chan, and K.M. Ho, Phys. Rev. Lett. **67**, 1454 (1991); **69**, 2452 (1992).

²⁴Y. Nakajima, G. Uchida, T. Nagao, and S. Hasegawa (unpublished).

²⁵S. Kono, K. Higashiyama, and T. Sagawa, Surf. Sci. **165**, 21 (1986).

²⁶G.V. Hansson and R.I.G. Uhrberg, Surf. Sci. Rep. **9**, 197 (1988).

²⁷Y. Hasegawa, I.-W. Lyo, and Ph. Avouris, Appl. Surf. Sci. **76-7**, 347 (1994).